

MILESTONE REPORT

DESIGN AND SIMULATION OF LAR READOUT ELECTRODE

MILESTONE: MS31

| | |
|-------------------------------|---------------------------------|
| Document identifier: | AIDAinnova-MS31 |
| Due date of milestone: | End of Month 23 (February 2023) |
| Report release date: | 30/03/2023 |
| Work package: | WP8: Calorimetry |
| Lead beneficiary: | CUNI |
| Document status: | Final |

Abstract:

The high granular liquified noble gas calorimeter for future colliders can be realised by finely segmented readout electrodes (multi-layer PCBs). The main scope of the project is the optimisation of the design, simulation, production and test of the multi-layer PCBs as readout electrodes which is discussed in the following.

AIDAInnova Consortium, 2023

For more information on AIDAInnova, its partners and contributors please see <http://aidainnova.web.cern.ch/>

The Advancement and Innovation for Detectors at Accelerators (AIDAInnova) project has received funding from the European Union's Horizon 2020 Research and Innovation programme under Grant Agreement no. 101004761. AIDAInnova began in April 2021 and will run for 4 years.

Delivery Slip

| | Name | Partner | Date |
|--------------------|--|----------------------|------------|
| Authored by | Roman Poeschl Roberto Ferrari Katja Kruger | CNRS INFN DESY | 15/03/2023 |
| Edited by | Sabrina El Yacoubi | CERN | 20/03/2023 |
| Reviewed by | Giovanni Calderini [Deputy Scientific coordinator] | CNRS | 25/03/2023 |
| Approved by | Giovanni Calderini [Deputy Scientific coordinator] Steering Committee | | 30/03/2023 |

TABLE OF CONTENTS

| | |
|--|-----------|
| 1. INTRODUCTION..... | 4 |
| 2. DESIGN OF THE CALORIMETER..... | 5 |
| 3. READOUT SYSTEM..... | 6 |
| 3.1 MULTILAYER ELECTRODES | 6 |
| 3.2 FULL READOUT CHAIN | 8 |
| 3.3 COLD ELECTRONICS..... | 9 |
| 4. PCB PROTOTYPES | 9 |
| 4.1 IJCLAB PROTOTYPES | 9 |
| 4.2. CERN PROTOTYPE..... | 11 |
| 5. REFERENCES..... | 12 |

Executive summary

The design of the liquified noble gas calorimeter was optimised for the requirements of electron-positron colliders. The geometry with inclined lead absorbers and liquid argon as active medium is considered as a baseline. Alternative geometries using liquid krypton or trapezoidal shape of the absorbers were investigated in order to improve the performance.

The simulations of the straight readout electrodes realised through a PCB with seven layers were performed using Finite Element Method. The goal of a crosstalk below 1% seems to be easily reachable, with the shaper considered, even without ground shields in the PCB design.

The electronic noise per cell in individual longitudinal layers was estimated considering the full readout chain. A signal-over-noise ratio of 5 to 10 could be achieved for minimum ionising particles and electronics sitting outside the cryostat.

The possibility of placing the electronics inside the cryostat is under study. The noise values per cell will drop by a factor of 5 to 10 in this condition. Careful considerations of the heat dissipation in the liquified noble gas medium and about the non-possibility of interventions on the electronics are needed.

First PCB prototypes were built at IJCLab and at CERN. The prototype at IJCLab allows for a deep understanding and tuning of the simulation software. Complementary, the prototype at CERN is a 1:1 model with different layouts in the towers (e.g. the number and width of the ground shields). The measurements with the CERN PCB prototype show a crosstalk below the target value of 1% as expected. The measurements with both prototypes show a qualitative agreement with the simulations, the work for an improved quantitative agreement is ongoing.

1. INTRODUCTION

The liquified noble gas calorimetry is a well proven concept used in numerous past and current high-energy-physics experiments (e.g. D0, H1, NA48, ATLAS). The main advantages of this technology are excellent energy and spatial resolution, very good linearity, stability and uniformity of the response, as well as radiation hardness. A new design optimised for advanced reconstruction techniques such as neural network reconstruction or particle flow was proposed for the Future Circular hadron-hadron Collider (FCC-hh) [1]. The concept is well suited also for future electron-positron colliders [2]. One of the key points for calorimeters at future electron-positron machines is the very precise measurement of energy with low systematics. Liquified noble gas calorimetry fulfils this requirement due to the stability of the response and hence the opportunity to achieve a very precise calibration. Another requirement is the measurement of electrons and photons with energies down to 300 MeV. This also leads to a challenging constraint on the electronic noise of the detector and limits the acceptable material budget in front of the calorimeter.

The proposed geometry of the liquified noble gas calorimeter allows for high granularity through the usage of the straight multilayer electrodes with fine segmentation (multilayer PCBs). The proposed

segmentation for the standard cells is based on 12 longitudinal compartments ($\Delta r = 3.5$ cm), with cell sizes from 8 mrad in $\Delta\phi$ and 10 mrad in $\Delta\theta$.

The electromagnetic calorimeter is also optimised for particle identification. The second layer with fine segmentation is designed for γ/π^0 separation. First studies using multivariate analysis show promising results with a 95% γ efficiency for about 10% of π^0 contamination in the whole energy range using simulations ignoring the electronic noise.

The design, simulation and production of PCB test modules is the main objective of the WP8.2.2 task. Special focus is given to the resulting signal attenuation, the capacitances of the signal channels, the crosstalk between different channels and the electronics noise per cell.

2. DESIGN OF THE CALORIMETER

An optimisation of the geometry for electron-positron colliders (e.g. FCC-ee) has been performed. The current baseline geometry consists of 1536 lead absorber plates inclined by 50.4° in the radial plane, as shown in Figure 1. The geometry is realised as a sandwich of lead absorbers (with a thickness of 2 mm), liquid argon (LAr, with a gap size of 1.2 – 2.4 mm) and readout boards (Printed Circular Board with a thickness of 1.2 mm) in the middle of the gap. Twelve longitudinal compartments are considered. The first compartment (the so-called presampler) is without lead absorbers in order to allow for a precise correction of the energy lost in the upstream material. The second compartment (the so-called strip layer) has a finer granularity in θ for π^0 / γ separation. The cell sizes under consideration are $\Delta r = 3.5$ cm, $\Delta\phi \geq 8$ mrad, $\Delta\theta = 10$ (2.5) mrad for the nominal (strip layer) cells. The total thickness of the active volume of the calorimeter is 40 cm corresponding to about 22 radiation lengths X_0 in the centre of the calorimeter. The calorimeter is placed inside an aluminium cryostat.

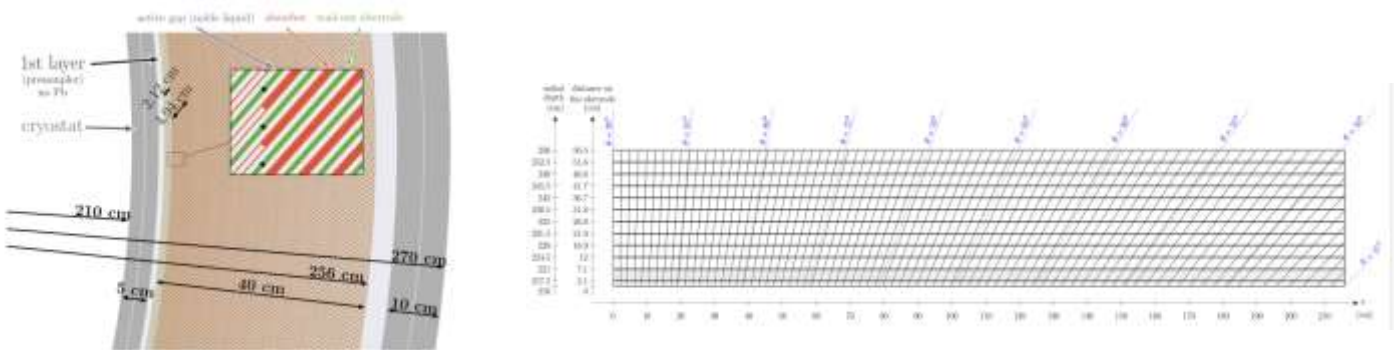


Fig. 1 Layout of the baseline geometry for the FCC-ee liquified noble gas electromagnetic calorimeter (left). The segmentation of the calorimeter (right).

The geometry description of the calorimeter is available in key4HEP [3]. The Geant4 energy deposits are merged into cells and calibrated accounting for the radially-dependent sampling fraction. The sampling fraction is derived separately for each longitudinal compartment. Two clustering algorithms (fixed size sliding window and variable size topo-clustering) are available for event reconstruction.

An energy resolution for electrons with a sampling term of 9% and a constant term of 0.7% is achieved with the baseline geometry.

Alternative geometries were studied in order to improve the performance of the calorimeter. The energy resolutions for different geometries are shown in Figure 2 (left). The option with liquid krypton (LKr) and lead plates keeping the same amount of X_0 as the baseline geometry seems promising, leading to a sampling term as good as 5%.

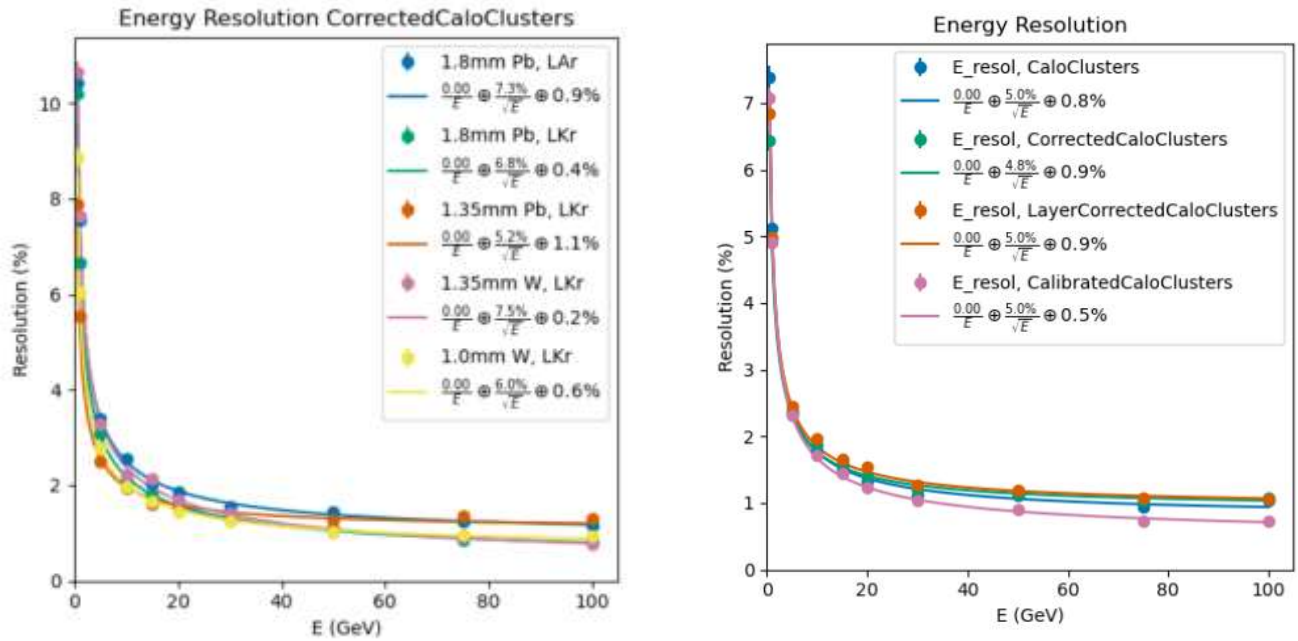


Fig. 2 Energy resolution of electrons for different geometry options under consideration. Results with straight absorbers (left) and with trapezoidal absorbers with LKr as active medium (right).

The sampling fraction is increasing with the radius in the current baseline geometry. An alternative option with a trapezoidal shape of the absorbers to keep the sampling fraction constant was investigated. This solution should improve the constant term in the energy resolution. The summary of the studies with lead absorbers and LKr as active medium are shown in Figure 2 (right). The results are shown for various methods of energy calibration. The use of multivariate regression techniques for energy reconstruction (pink line) leads to an improved constant term in the resolution. The mechanical realisation of a design with trapezoidal absorbers might be challenging and is under study.

3. READOUT SYSTEM

3.1 MULTILAYER ELECTRODES

The readout of the calorimeter will be performed through straight multilayer electrodes. The current design is based on a 1.2 mm thick Printed Circuit Board (PCB) consisting of 7 layers as shown in Figure 3 (right). The high-voltage layers create an electric field in the liquified noble gas gap of the detector. The signal pads, located in the layer below, collect the ionisation signal which is extracted to either the back or the front of the electrode through the signal traces as indicated in Figure 3 (left). In between the pads and the traces, there is a layer of shields that minimise the crosstalk from the

pads to the signal traces connected to different pads. Two signal pads are connected to a signal trace by vias inside the PCB.

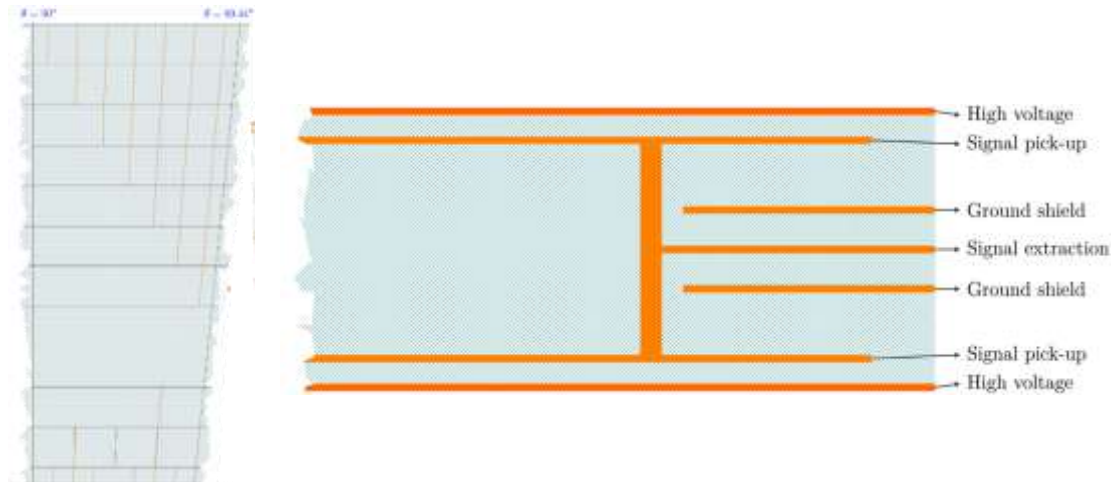


Fig. 3 The layout of the PCB. The readout of one tower in a scale 10:1 (left). The transverse view of the PCB (right).

Finite Element Method (FEM) simulations of the electrode were performed using the Ansys HFSS 3D layout [3]. The signal attenuation and the crosstalk induced on other cells in the same tower were estimated. The results for the simulations with no shields and no signal shaping are shown in Figure 4. The peak value of the transmitted current reaches about 93% of the injected signal.

The highest crosstalk is observed in the direct neighbouring cell (cell 6 in the numbering scheme introduced in Figure 4 left) as expected. The crosstalk is visible also in other cells of the tower (cell 5, 4 and 1 due to transmission line/pad coupling, cell 2 and 3 from indirect coupling). The crosstalk can be suppressed with the insertion of ground shields and with signal shaping.

A peak-to-peak crosstalk below 1% seems to be easily achievable for a signal shaping time larger than 100 ns even without ground shields as shown in Table 1. A shorter shaping time will be possible adding one or two ground shields, options under consideration.

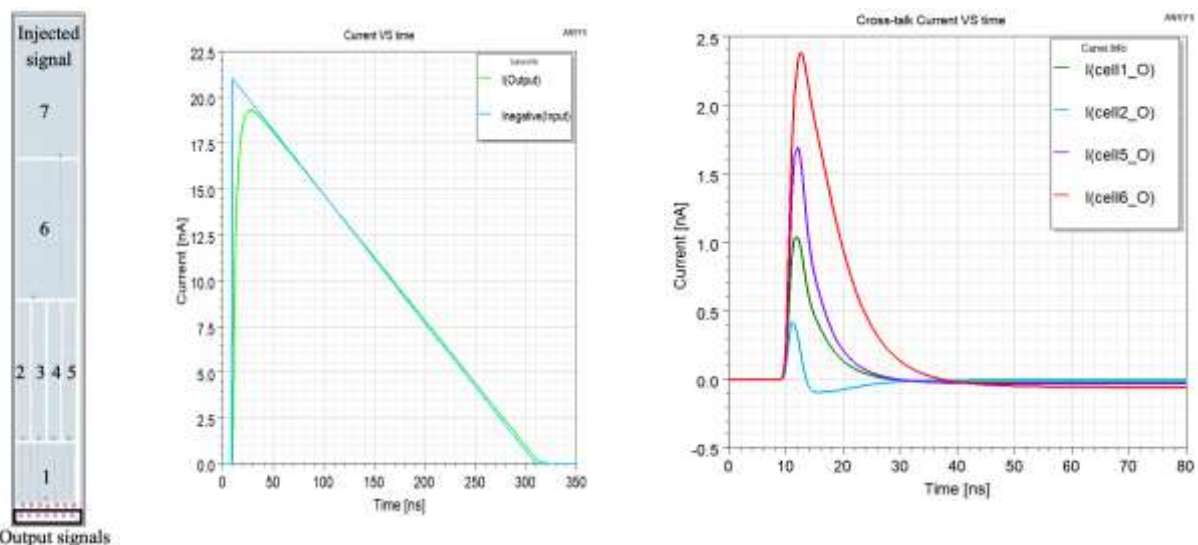


Fig. 4 A scheme of the cells' numbering (left). Results of the FEM simulations without shields and without signal shaping for the injected signal (middle) and crosstalk (right).

| 2 shields | | | | | | |
|---------------------|--------|--------|--------|--------|--------|--------|
| Cross-talk (%) | Cell 1 | Cell 2 | Cell 3 | Cell 4 | Cell 5 | Cell 6 |
| Shaping time (ns) ↓ | | | | | | |
| No shaper | 0.54 | 0.85 | 0.85 | 2.31 | 2.62 | 9.11 |
| 20 | 0.03 | 0.04 | 0.01 | 0.09 | 0.11 | 0.75 |
| 50 | 0.01 | 0.02 | 0.0 | 0.04 | 0.05 | 0.37 |
| 100 | 0.01 | 0.01 | 0.0 | 0.02 | 0.03 | 0.23 |
| 150 | 0.0 | 0.01 | 0.0 | 0.02 | 0.02 | 0.18 |
| 200 | 0.0 | 0.01 | 0.0 | 0.01 | 0.02 | 0.15 |
| 300 | 0.0 | 0.0 | 0.0 | 0.01 | 0.01 | 0.13 |

| 1 shield | | | | | | |
|---------------------|--------|--------|--------|--------|--------|--------|
| Cross-talk (%) | Cell 1 | Cell 2 | Cell 3 | Cell 4 | Cell 5 | Cell 6 |
| Shaping time (ns) ↓ | | | | | | |
| No shaper | 2.42 | 0.82 | 0.87 | 3.86 | 4.14 | 10.36 |
| 20 | 0.4 | 0.05 | 0.04 | 0.58 | 0.58 | 1.72 |
| 50 | 0.18 | 0.02 | 0.01 | 0.26 | 0.26 | 0.79 |
| 100 | 0.1 | 0.01 | 0.0 | 0.14 | 0.14 | 0.45 |
| 150 | 0.07 | 0.01 | 0.0 | 0.11 | 0.11 | 0.34 |
| 200 | 0.06 | 0.0 | 0.0 | 0.09 | 0.09 | 0.28 |
| 300 | 0.05 | 0.0 | 0.0 | 0.07 | 0.07 | 0.23 |

| 0 shield | | | | | | |
|---------------------|--------|--------|--------|--------|--------|--------|
| Cross-talk (%) | Cell 1 | Cell 2 | Cell 3 | Cell 4 | Cell 5 | Cell 6 |
| Shaping time (ns) ↓ | | | | | | |
| No shaper | 6.27 | 2.6 | 3.2 | 8.75 | 8.61 | 15.96 |
| 20 | 0.7 | 0.1 | 0.1 | 0.99 | 0.92 | 2.58 |
| 50 | 0.3 | 0.02 | 0.02 | 0.43 | 0.4 | 1.14 |
| 100 | 0.17 | 0.01 | 0.01 | 0.24 | 0.23 | 0.64 |
| 150 | 0.13 | 0.01 | 0.0 | 0.18 | 0.17 | 0.48 |
| 200 | 0.1 | 0.01 | 0.0 | 0.15 | 0.14 | 0.4 |
| 300 | 0.08 | 0.0 | 0.0 | 0.12 | 0.11 | 0.32 |

Table 1: Peak-to-peak crosstalk in % for various shaping times and a different number of ground shields.

3.2 FULL READOUT CHAIN

The complete readout chain was studied using an analytical description. The cell capacitances estimated using FEM simulations were used together with different signal extraction strategies and front-end electronics scenarios. The electronic noise for an option with two ground shields, a charge preamplifier with $e_n = 0.5 \text{ nV} / \sqrt{\text{Hz}}$ and $i_n = 1 \text{ pA} / \sqrt{\text{Hz}}$ followed by a $CR^2 - RC^2$ shaper featuring a shaping time of 200 ns, followed by 5 m of 100 Ω coax cable, is shown in Figure 5 (left). An average signal-over-noise ratio for a minimum ionizing particle (MIP) between 5 and 10 is reached, as shown in Figure 5 (right).

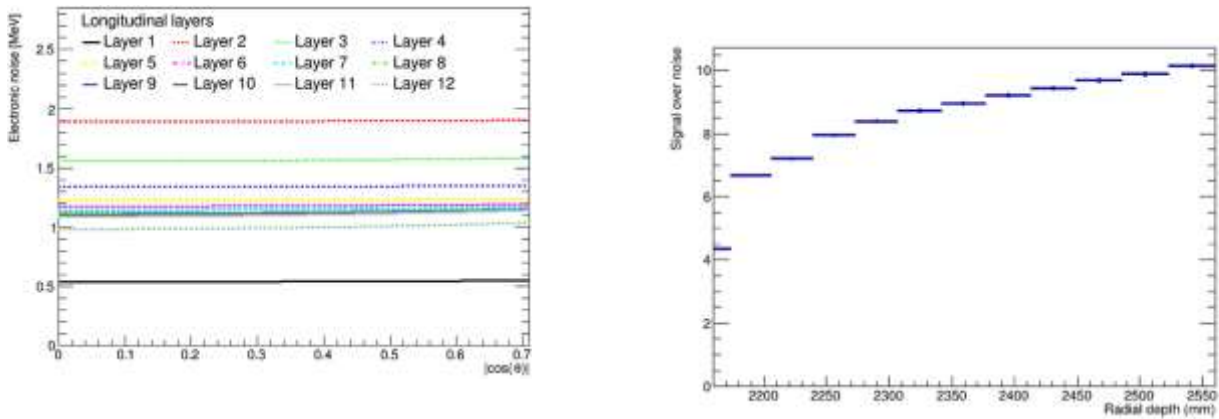


Fig. 5 Electronic noise per cell (in MeV) in individual longitudinal compartments as a function of the polar angle (left). Average signal-over-noise ratio per longitudinal compartment for a MIP (right).

3.3 COLD ELECTRONICS

An alternative approach to the so-called warm electronics (discussed above) is the cold electronics. The readout electronics situated fully or partially inside the cryostat is considered as an alternative approach. First simulations show a reduction of the noise levels of 5 to 10 times compared to the warm electronics. Two main considerations are to be carefully evaluated. First, the usage of the cold electronics will not allow for repairs of electronics failures. Another critical point could be the heat dissipation in the liquified noble gas which is to be studied. A simple setup with HGCROC [5] front-end readout ASIC in liquid nitrogen has been used at IJCLab to perform the first tests.

4. PCB PROTOTYPES

Real prototypes are necessary for a deeper understanding of the simulations and especially for the development of the design of the calorimeter readout. First prototypes of PCBs were prepared at IJCLab and at CERN.

4.1 IJCLAB PROTOTYPES

First simple prototypes, one with a single microstrip line and another with two coupled matched microstrip lines, were built at IJCLab, as shown in Figure 6 (left). Measurements of the scattering matrix S -parameters were performed and translated into impedance and attenuation factors. The results show good agreement between simulations (with FEM Cadence Allegro [6] and Sigroty [7]) and measurements for frequencies up to 100 MHz.

A second prototype with the size of 10 cm x 15 cm consists of 3 x 2 cells (scheme on Figure 6 right). The model was built to measure detailed properties of the cells and crosstalk. The parameters of the PCB were tuned to have an impedance of 50 Ω . Due to manufacturing constraints a model with an even number of layers was constructed with a double trace stripline. The prototype was built without the high voltage layers.

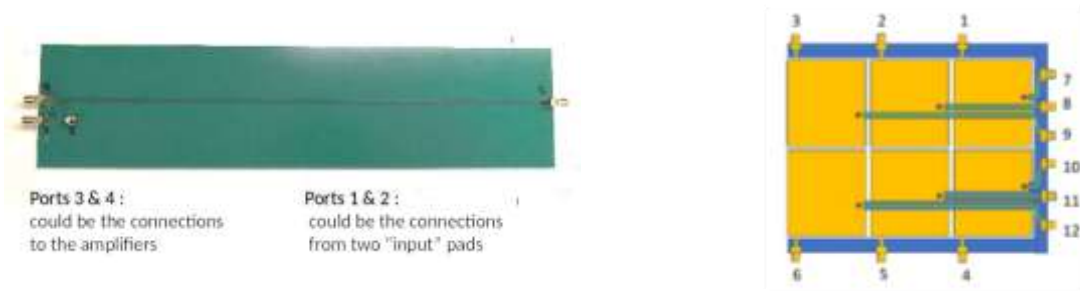


Fig. 6 PCB prototype 1 (left) and prototype 2 (right) at IJCLab . The numbering of the input/output connections is shown for prototype 2.

The signal was injected in one cell (input 1) and the crosstalk signals on the other cells were measured. A capacitive crosstalk on neighbouring cells from the other tower was observed. Also mainly inductive crosstalk on other cells in the same tower was observed. The results are summarised in Figure 7. The agreement between measurements and simulations (using the model of the PCB extracted from the Cadence design by the Sigrity tool) is good for nearby channels. The crosstalk measured on the far channels (channels 5 and 6) is the result of both capacitive and inductive effects. This sub-per-mille effects are less accurately described by the model of the PCB.

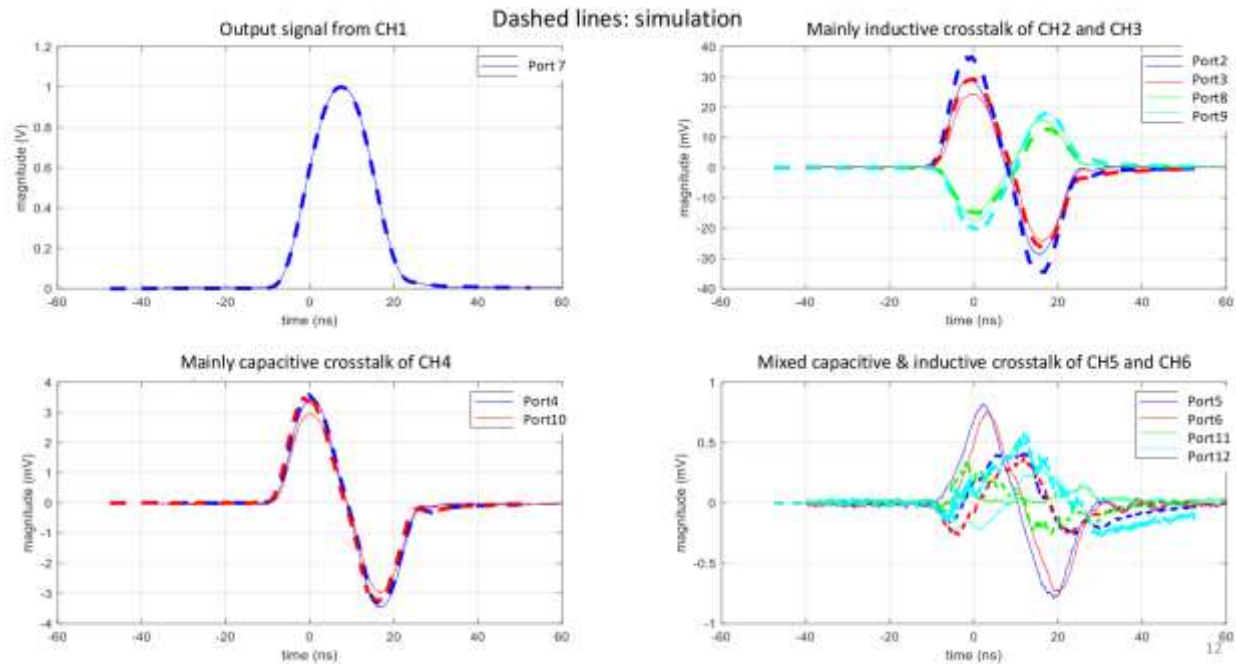


Fig. 7 Measurements of the crosstalk at IJCLab. The numbering scheme is shown in Figure 6 (right). The dashed lines correspond to the simulations.

The total capacitance, inductance and coupling parameters per channel were extracted from the measurements. Using a simpler model of the PCB instead of the full Sigrity model, capacitive measurements can still be reproduced, which allows to determine the global pad + strip capacitance. The mutual inductances can be obtained with a similar method, although with more uncertainties on the validity of the simple model used. Moreover, a detailed measurement of the coupling capacitance was performed.

4.2. CERN PROTOTYPE

The PCB prototype with 7 layers prepared at CERN is a 1:1 scale model with the size of 58 cm x 44 cm x 1.2 mm (Figure 8). The model contains 16 θ -towers with different setups (e.g. different number and widths of the ground shields).

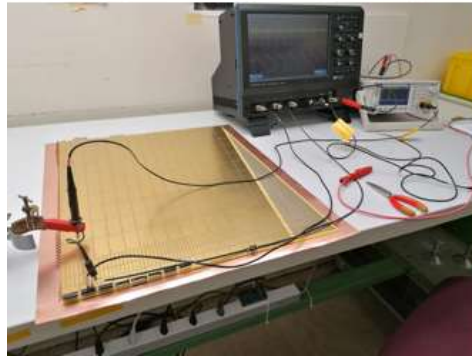


Fig. 8 Experimental setup with the PCB prototype at CERN

A triangular input signal was injected in cell 7 (the numbering is shown in Figure 4 left) and the response in the inner cells in the same tower was extracted using a 50 Ω readout probe. Results for measurements with one ground shield are shown in Figure 9. Overall, the results of the measurements qualitatively agree with the simulations. The highest crosstalk is observed in the neighbouring cell (cell 6) as expected. The insertion of ground shields mitigates the crosstalk. The measurements confirm that a crosstalk below 1% could be easily achieved even without shielding. This is also valid for the strip layer where a strip-to-strip crosstalk below 1% could be reached with the shaper under consideration. A ground trace located between the cells mitigates the crosstalk in the strip layer as predicted by the simulations. The agreement between measurements and simulations is still to be improved, especially for small signals and short shaping times.

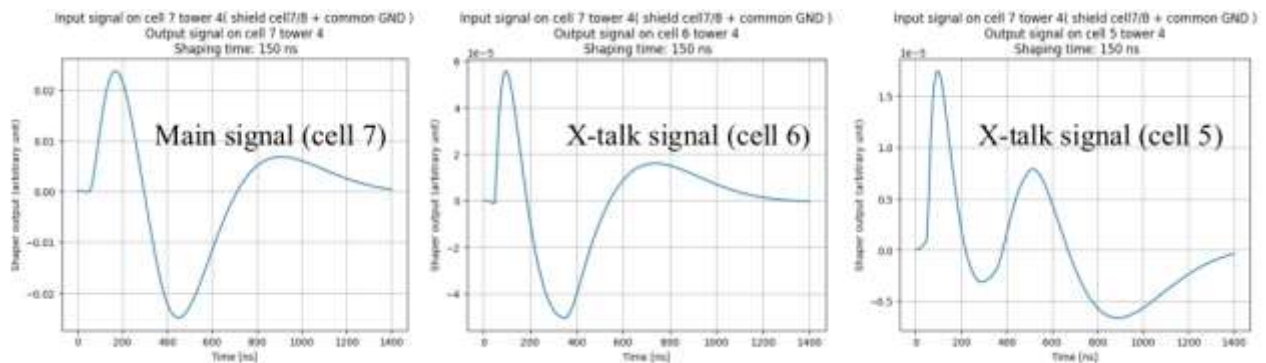


Fig. 9 Measurements of the crosstalk with the CERN PCB prototype with one shield and the signal injected in cell 7 with a 150 ns shaper CR-RC² emulation (the cell numbering scheme is shown in Figure 4 left).

5. REFERENCES

- [1] M. Aleksa, P. Allport, R. Bosley, J. Faltova, J. Gentil, R. Goncalo, C. Helsens, A. Henriques, A. Karyukhin, J. Kieseler, C. Neubüser, H.F.P. Da Silva, T. Price, J. Schliwinski, M. Selvaggi, O. Solovyanov, A. Zaborowska (2019), *Calorimeters for the FCC-hh*, Tech. rep., CERN, arXiv:1912.09962, <https://cds.cern.ch/record/2705432>.
- [2] M. Aleksa, F. Bedeschi, R. Ferrari, F. Sefkow, C.G. Tully, (2021), *Calorimetry at FCC-ee*, *Eur. Phys. J. Plus* 136 (10) (2021) 1066, <http://dx.doi.org/10.1140/epjp/s13360-021-02034-2>.
- [3] G. Ganis, C. Helsens, V. Völkl (2021), *Key4hep, a framework for future HEP experiments and its use in FCC*, <http://dx.doi.org/10.48550/ARXIV.2111.09874>.
- [4] G.J. DeSalvo, J.A. Swanson, ANSYS Engineering Analysis System User's Manual, Swanson Analysis Systems, 1985, Houston, Pa., 1985, URL <https://search.library.wisc.edu/catalog/999581007202121>
- [5] F. Bouyjou, G. Bombardi, F. Dulucq, A. El Berni, S. Extier, M. Firlej, T. Fiutowski, F. Guilloux, M. Idzik, C. De La Taille, A. Marchioro, A. Molenda, J. Moron, K. Swientek, D. Thienpont, T. Vergine (2022), *HGCROC3: the front-end readout ASIC for the CMS High Granularity Calorimeter*, JINST 17 (2022) 03, C03015
- [6] Cadence (2023), https://www.cadence.com/en_US/home/tools/pcb-design-and-analysis/pcb-layout/allegro-pcb-designer.html [Accessed 15th February 2023].
- [7] Cadence (2023), https://www.cadence.com/ko_KR/home/tools/pcb-design-and-analysis/si-pi-analysis/sigrity-aurora.html [Accessed 15th February 2023].